Chapter 5
Print ISBN: 978-81-976653-9-4, eBook ISBN: 978-81-976653-5-6

Evolution of 2007-08 Madden-Julian Oscillation (MJO07-08) Passing Over the New Guinea Highlands (Part II): Effects of Mechanical and Thermal Forcing on the Modification of Heavy Orographic Rain

Justin G. Riley [a,b] and Yuh-Lang Lin [a*]

DOI: https://doi.org/10.9734/bpi/crpps/v2/296

Peer-Review History:
This chapter was reviewed by following the Advanced Open Peer Review policy. This chapter was thoroughly checked to prevent plagiarism. As per editorial policy, a minimum of two peer-reviewers reviewed the manuscript. After review and revision of the manuscript, the Book Editor approved the manuscript for final publication. Peer review comments, comments of the editor(s), etc. are available here: https://peerreviewarchive.com/review-history/296

ABSTRACT

In Part II of a series of studies on the evolution of airflow and precipitation associated with the 2007-08 Madden-Julian Oscillation (MJO07-08) over the New Guinea Highlands (NGH), we focus on how the mechanical and thermal forcings affecting the enhancement and the essential ingredients of heavy orographic rain. In this study, the mechanical and thermal forcing effects of the NGH on MJO07-08's propagation and rainfall over the island of New Guinea are investigated by adopting the Advanced Research Weather Research and Forecasting (WRF) model. It is found that both forcings affect the propagation of MJO07-08, which lead to heavy orographic rainfall production with the mechanical forcing of NGH playing a stronger role in the orographic blocking than the thermal forcing. In addition, it is found that there are two flow regimes associated with MJO07-08 over the NGH: (1) the *flow-around regime* and (2) the *flow-over regime*. In the *flow-around regime*, the convective system associated with the MJO split into two while passing over the NGH due to the strong orographic blocking and this flow regime occurs when the mountain height is approximately above 50% of the original mountain height. In this flow regime, the orographic rainfall increases as the mountain height increases. Based on a series of systematic sensitivity tests, the *flow-over regime* occurs when the mountain is approximately below 50% of the original mountain height. Finally, it is found that the essential orographic rain ingredients associated with the MJO07-08 event are like those associated with TCs over a mountain. With a series of sensitivity tests with varying mountain

[a] North Carolina A&T State University, Greensboro, North Carolina, USA.
[b] NOAA Cooperative Institute for Great Lakes Research (CIGLR), Ann Arbor, Michigan, USA.
**Corresponding author: E-mail: ylin@ncat.edu;*

height, it is found that once the mountain height reaches 75% of the original height of the NGH, the maximum rainfall amount starts to decrease as the mountain height reaches approximately 75% of the original height.

Keywords: Madden-Julian Oscillation (MJO); orographic rain; New Guinea Highlands (NGH); common ingredients.

1. INTRODUCTION

The Madden-Julian Oscillations (MJOs) have enormous impacts on the weather systems around the world, which plays a vital role in the intra-seasonal predictions across the globe [1]. An example of this is when an MJO moves through the Maritime Continent (MC), its propagation and rainfall are strongly influenced by the orography of MC islands [2-6]. During the MJO's propagation, it is often blocked and weakened, causing the MJO convective system to break down and disappear. This is often called the "*barrier effect of the MC*" [3,7-10]. However, most previous studies on the propagation and rainfall of MJOs are based on global observational data and model simulations. Since the horizontal resolution of the data simulated by global models is coarse, such as 60 km, there is a need to examine the airflow and precipitation evolution at finer spatial and temporal resolutions.

In Part I of this series of studies on the evolution of airflow and precipitation associated with the 2007-08 Madden-Julian Oscillation (MJO07-08) past New Guinea Highland (NGH), [11] denoted as Part I or L20 hereafter) studied the orographic effects on the propagation and rainfall modification of MJO07-08 past the NGH and found that it goes through the blocking, splitting, and merging stages. During the *blocking stage*, the propagation of the MJO is slowed, which lead to the flow split at the northwest tip of the Guinea Mountains and the MJO convection split into two convective systems while passing over the NGH thus entering the *splitting stage*. The splitting stage is followed by the *merging stage* at the southeast corner of the NGH when the split flow and convective systems merge into one system, which behaves as the original MJO system. One deficiency in Part I [11] is the lack of thermal forcing in the planetary boundary layer considered, it remains to be explored. In addition, Part I focused on the propagation and structure changes of the precipitating system without considering the orographic rainfall mechanisms, such as the effects of diurnal thermal forcing associated with the orography on the MJO, the enhancement of orographic rain associated with MJO's past the NGH, and the essential ingredients of orographic rainfall.

In previous studies [8], the MJOs over the Maritime Continent (MC) are classified into two distinct groups: (a) MJO-C: the MJO propagates over the MC continuously, and (b) MJO-B: the MJO behaves differently from MJO-C, the MJO is blocked by the MC. Zhang and Ling [8] found that MJO-B's rainfall is much higher over the ocean than over the land. On the other hand, the MJO-C's rainfall over the ocean is not significantly higher than that over the land, indicating that the MC is inhibiting convective development over the ocean could be a possible mechanism for the MC's barrier effect. Therefore, it is proposed that the rainfall over the ocean is caused by the land/sea breeze associated with the islands. Ling et al. [9] investigated the effect of the diurnal cycle inland convection on the propagation of

the MJO over the Maritime Continent Convective Diurnal Cycle (MACCC) mechanism, i.e., the diurnal cycle inland convection acts as an intrinsic barrier effect on MJO propagation over the MC. Precisely speaking, the barrier effects should include both mechanical blocking effect and diurnal thermal forcing effects. In the studies of Zhang and Ling [8] and Ling et al. [9], however, they only focused on diurnal thermal forcing effects. Thus, there is a need to differentiate these two forcing mechanisms on the MJOs. In this study, we would like to investigate their relative contributions on the MJO07-08 when it passes over the NGH was not investigated, which deserves to be studied.

Based on the above discussions, in this study, we would like to address: (a) What impacts of the diurnal thermal forcing on the orographic rainfall propagation and modification? (b) what are the relative contributions between orographic blocking and diurnal thermal forcing on the MJO07-08 while it passes over the NGH? In this study, we will conduct mesoscale model simulations with sensitivity tests to differentiate these two forcings, such as removing the mountains and deactivating the diurnal heating and cooling. In addition, the modification of orographic rain associated with MJO07-08 will be investigated to understand how much the NGH enhances or weakens the orographic rain as an MJO passes over the island. Lin [12] shows that the enhancement mechanisms of orographic precipitation are extremely complicated and are highly dependent on multiple factors. To study this, we will remove the mountain (NoMT) and conduct sensitivity tests by varying mountain heights and comparing them with the control case (CNTL).

In addition, we would like to inspect moist flow regime change during MJO07-08's passage over the NGH. For example, Chu and Lin [13] found that there are three moist flow regimes for a conditionally unstable flow over an idealized 2D mountain: (1) An upstream-propagating convective precipitation system, (2) A quasi-stationary convective system over the mountain, and (3) A quasi-stationary convective system in the vicinity of the mountain peak along with the downstream-propagating convective system. The above moist flow regimes are controlled by the basic-flow speed (U), the mountain height (h), and the upstream moist Brunt-Vaisala frequency (N_w) of the environmental flow parameters, which could be represented by one nondimensional, moist Froude number, $F_w = U/(N_w h)$. In extending Chu and 'Lin's study, Chen and Lin [14] adopted the upstream unsaturated moist Froude number [15], $N_w^2 = (g/\theta)(\partial\theta_v/\partial z)$, where g is the gravitational acceleration, and θ_v is the virtual potential temperature to avoid negative values. Chen and Lin [14] included the convective available potential energy (CAPE) in addition to the moist Froude number (F_w). They identified four conditional unstable flow regimes over an idealized 2D mountain. The above interplay explains the flow characteristics among the orographic blocking, the precipitation system's advection, and the density current forcing. Their results found that under a low-CAPE flow, large horizontal wind speeds could modulate the orographic precipitation. Their findings imply that the precipitating system does not require a high CAPE to produce heavy orographic rainfall [16]. However, in our study, we need to revisit the previous studies for a three-dimensional flow over an isolated mountain.

The four flow regimes found in Chen and Lin [14] were extended by Chen et al. [17] to examine the flow regimes over a three-dimensional (3D) mountain with the inclusion of F_w and h/a (mountain aspect ratio, where a is the mountain half-width). Miglietta and Rotunno [18] conducted a series of simulations with a conditionally unstable flow impinging on a mesoscale ridge on a 3D domain and a relatively higher resolution to resolve cellular-scale features properly. Their found that the characteristics of the overall flow are similar to those in Chu and Lin [13]. They also proposed that a functional dependence of the rainfall rate was caused by three parameters: the triggering and orographic forcing of the convection and the convective time scales' advection ratio. Although the above-mentioned studies provided significant insight of the dynamics of conditionally unstable flow over idealized mountains, in this study we will try to understand the evolution of MJO07-08's propagation and its associated precipitation while passing over the NGH in a more realistic, complicated environments.

Another scientific problem we would like to address is to distinguish between flow-over and flow-around precipitating systems, as found in Smolarkiewicz and Rotunno [19]. Based on numerical studies, Buzzi et al. [20] demonstrated that reducing effective static stability of a moist low by latent heating may go through the regime transition from flow-around a higher mountain ridge to flow-over lower mountain ridge. Part I's [11] WRF simulation of MJO07-08 over NGH also showed that the splitting stage corresponds to the flow-around regime. However, their mesoscale model simulations do not update the sea surface temperature (SST) after the initialization. Updating the SST every 12 or 6 hours in the model simulations could improve the results of Part I [11]. This could also help obtain a better result for enhancing the MJO precipitation. A much finer model resolution may also be needed to obtain a much more detailed flow and precipitation fields to reveal the orographic effect. However, this does not mean that the 5km resolution model cannot capture the orographic enhancement of the NGH on MJO as it passes over the NGH.

Since MJO07-08 enters the blocking stage when it approaches the northwest (NW) corner of New Guinea, it is important to address the orographic impacts on the orographic rainfall (orographic initiation and enhancement) at the NW corner of the island New Guinea. The orographic forcing on incoming airstream is highly dependent on the detailed geometry of the mountain [12]. Therefore, the geometry of the mountain can affect the amount and distribution of orographic precipitation. The terrain geometry can greatly influence orographic precipitation in multiple ways, such as small-scale orographic features, large-scale terrain shape, and three-dimensional flow blocking and splitting [12]. To investigate the orographic impacts of the NGH on MJO, we will compare the airflow pattern and rainfall amount and distribution in response to the variation of slope heights and mountain geometry. Lin [12] showed that the amount and distribution of the orographic tropical cyclone (TC) precipitation are strongly dependent on the TC's synoptic environment during its passage over a mountain range. In this study, we will explore whether this idea is applicable to MJO. To help us understand the orographic influence on rainfall on the NW corner of New Guinea, we will help us with the ingredient approach discussed in Lin et al. (2001). The following equation determines the orographic precipitation (P):

$$P = \varepsilon\left(\frac{\rho_a}{\rho_w}\right)(V_H \cdot \nabla h + w_{env})\left(\frac{L_s}{c_s}\right)q_v,$$

where ρ_a and ρ_w are the air density and the liquid water density and, respectively, ε is the precipitation efficiency, w_{oro} and w_{env} are the vertical velocities forced by orography and environment, respectively, q_v is the water vapor mixing ratio, L_s and c_s are the horizontal scale of the precipitating system and its moving speed, respectively. To examine the ingredients of orographic rainfall of the NW corner of the NGH, we will be using the 1km resolution, mesoscale model. This will allow us to take a closer look than using the 5km resolution model. The 5km resolution model used in Part I [11] looks at the mechanical and diurnal effects of the NGH on MJO. Still, we believe we need to use a finer resolution to study the orographic ingredients.

Based on Eq. (1), Lin et al. (2001) proposed the common ingredients for heavy orographic rainfall: (1) there needs to be strong vertical motion (w) at the mountain's slope. (2) There must be high CAPE in the convective system, and finally (3) the mountain itself must have a high peak. However, large w requires high mountain and high CAPE. This means that there will be a point where there is maximum rainfall at a certain height. This means after that certain mountain height, we would see a plateau or a decrease in the amount of orographic rainfall. When looking at the accumulated rainfall along the upslope and downslope of the mountain compared to the varying mountain height, we can see exponential growth in rainfall accumulated while the mountain height is between no mountain and 50 percent of the original mountain.

In this study, we will use the WRF model [21] to examine the orographic and thermal effects of the NGH on MJO propagation and rainfall over the island of New Guinea. First, we will discuss the model description and experimental design in section 2. This will also include the model verification of each of the sensitivity cases. Next, we examine our simulations' results, looking at the mechanical and diurnal thermal forcing associated with the orography on MJO, the enhancement of orographic rain associated with MJO passing over the NGH, and the ingredients of orographic rainfall on the NW corner of the NGH in sections 3, 4, and 5, respectively. Finally, we will be presenting the concluding remarks of our study in section 6.

2. MODEL DESCRIPTION, NUMERICAL EXPERIMENT DESIGN, AND MODEL VERIFICATION

2.1 Model Description

The WRF model version 3.9.1 [21] is adopted for the numerical simulations of MJO07-08 and the associated rainfall and propagation over the NGH. The WRF model is a numerical weather prediction system developed to help with better mesoscale weather. The WRF model incorporates initial idealized data or better forecasting weather by incorporating initial real data into the model. The WRF model is a three-dimensional, non-hydrostatic, fully compressible model that uses

terrain-following vertical coordinates with stretched grid resolution, one or two-way multiple-nesting capability, options for upper and lateral boundary conditions, etc. The WRF model governing equations are written in flux-form with conserved mass and dry entropy. Thus, the WRF model provides a flexible and robust platform for operational forecasting while offering more options in the advanced scheme in physics parameterizations and numerical methods, including data assimilation techniques.

2.2 Numerical Experiment Design

For the first mesoscale simulation (CNTL) performed in this study, the domain is the same as in Part I (L20), which includes the island of New Guinea and its surrounding areas. The CNTL simulation contains only one domain, which expands from the southwest corner at (122ºE, -15ºS) to northeast corner at (162ºE, 2ºN) and consists of 887 x 376 horizontal grid points with 5km horizontal grid resolution. There are 32 vertically stretched grid levels and 30 s time interval. The domain and NGH terrain are shown in Fig. 1. The domain is designed so that the whole MJO event of MJO07-08 passing over the NGH as described in Part I [11] and NGH are entirely included and well resolved, so that the NGH impacts the MJO can be simulated in more detail. The physics parameterization schemes selected for the simulations are summarized in Table 1.

Table 1. Parameterization schemes used for physical processes

Physical Process	Parameterization Scheme
Cumulus Convection	Grell 3D Scheme
Microphysics	WSM6
Planetary boundary layer	YSU
Longwave radiation	RRTM
Shortwave radiation	RRTMG

Details of the schemes can be found in the WRF user's manual [21]. Unlike the global model simulations conducted in previous studies, the combination of the domain, grid resolution, and physics parameterization schemes allow us to study mesoscale dynamics associated with the passage of the MJO07-08 over the NGH. The WRF model is initiated with ECMWF ERA-Interim reanalysis data [22] for 6 days (12/29/00Z/07-1/4/00Z/08), which includes the period the MJO07-08's passage of the NGH. Several sensitivity cases are summarized in Table 2 of section 3, which are designed to address the questions raised in this study, as discussed in section 1.

2.3 Model Verification

The experimental design of the first case for this study (Part II) is based on the mesoscale simulation that is described in Part I [11]. However, unlike Part I, we update the SST data every 6 hrs after the model's initiation. In addition, the WRF model does not predict the SST during the simulation, meaning updating the SST during the simulation will give provide us a more accurate prediction of the environment while the MJO07-08 propagates over the NGH. The SST is also updated in all the CNTL and sensitivity tests.

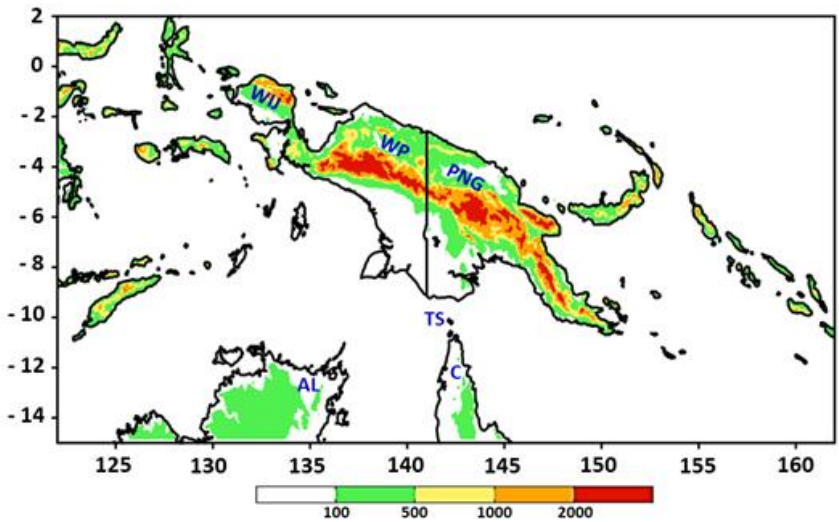

Fig. 1. The model domain and topography of New Guinea Highland (NGH) extend from northwest of New Guinea to the southeast with the highest peak of 4884 m. The terrain height is in m. The topography of regions denoted in this domain is WP: West Papua; WIJ: West Irian 679 Jaya (northwest peninsula of the West Papua); PNG: Papua New Guinea; PNG: Papua New Guinea; AL: The Arnhem Land of Australia; C: Cape York Peninsula of Australia and TS: Torres Strait

The WRF-simulated CNTL result is verified by comparing it with the tropical rainfall measuring mission (TRMM) 3B42 Version 7 data, the NOAA-Interpolated OLR data, and wind vector field data. For the TRMM data, the temporal resolution used is 3-hour data from 12/30/07 to 1/4/08 with a spatial resolution of 0.25° latitude-longitude grid. The NOAA-Interpolated OLR data is from 12/30/07 to 1/4/08 with a temporal resolution of 1 day and a spatial resolution of 2.5° latitude-longitude grid.

Verification of the model simulated MJO passing over the NGH includes precipitation, total water content, and outgoing longwave radiation (OLR). When comparing the CNTL simulated rainfall fields to those of Part I [11] (Fig. 2), the CNTL results show slightly more rainfall along the NGH and the coast during the blocking stage MJO07-08. When comparing the results to TRMM, their rainfall patterns are similar in the same period. When comparing the rainfall from the CNTL case to Part I [11] and the TRMM data, the CNTL case, which updated SST data, improves the MJO event's model simulation. There is only a slight increase in rainfall in the simulation. However, the rainfall pattern seen in the TRRM observational data results is also present in the CNTL case. This indicates that updating the SST data has improved the simulation of rainfall structure.

The simulated OLR fields (Fig. 3) are slightly stronger in the number of deep clouds along the NGH compared to that in Part I [11]. During the blocking stage, such as at 12Z, 12/31/07, a large deep convection cloud forms on the southwest side of the island of New Guinea, compared to Part I. However, during the simulation run of the CNTL case, that large deep cloud does not form in that island area. The OLR pattern is like the pattern shown in the OLR observational data (Fig. 3). These are present when looking at all three stages that MJO07-08 goes through during its eastward propagation. Updating the SST data also helps simulate the deep convective clouds associated with MJO07-08 and produce results like the OLR observational data. The verification of the CNTL case shows that updating the SST data during the simulation every 6 hours improved the results as shown in Part I. Thus, the simulations are appropriate to be used for this study.

3. MECHANICAL AND THERMAL FORCINGS ON MJO07-08 DURING ITS PASSAGE OVER NGH

It is found [23] that during its passage of the island of New Guinea, MJO07-08 is split into two convective systems along the northeast and southwest coasts, respectively (Fig. 4). Once MJO07-08 lands on the island, it reappears to the southeast of New Guinea. Thus, the MJO passes over the NGH approximately from 12/31/07 – 1/5/08.

From 12/21/07 – 1/10/08, 07-08 appears to jump over the MC instead of moving smoothly over it, in a way like typhoons passing over Taiwan's Central Mountain Range [12]. As MJO07-08 propagates over the island of New Guinea, it appears to be blocked by the NGH before passing through the three stages found in Part I [11] and then continuing its eastward propagation. As shown in Fig. 1, it takes over a month (12/01/07 - 01/10/08) for the MJO to pass over the island and NGH completely, during which the MJO07-08 goes through the blocking, splitting, and merging stages. In this study, we will focus on the mechanical and thermal forcing during the blocking and splitting stages.

Since the blocking of MJO07-08 is caused by both the mechanical and thermal forcings of NGH, it is important to differentiate them. The mechanical forcing is caused by the blocking of the terrain of NGH on the propagation of the MJO while passing over it. The thermal forcing is caused by the diurnal heating or cooling of the island, which leads to the sea and land breezes. To differentiate the mechanical and thermal forcing of the NGH on the MJO, we perform three sensitivity tests to investigate the impacts of each forcing.

In the first sensitivity test, the terrain is removed (NMTN). The NoMT case will help us understand how important the mechanical forcing of the NGH impacts on the MJO as it passes over the island. As discussed in Part I [11], MJO07-08 goes through three stages as it propagates over the NGH. The first stage was the *blocking stage*, where the MJO is being blocked by the mountains, causing the southeastward movement to stall and discontinue. The second stage is the *splitting stage*, where the MJO splits into two separate convective systems, and the MJO flows around the NGH. Finally, the two convective systems merge into one

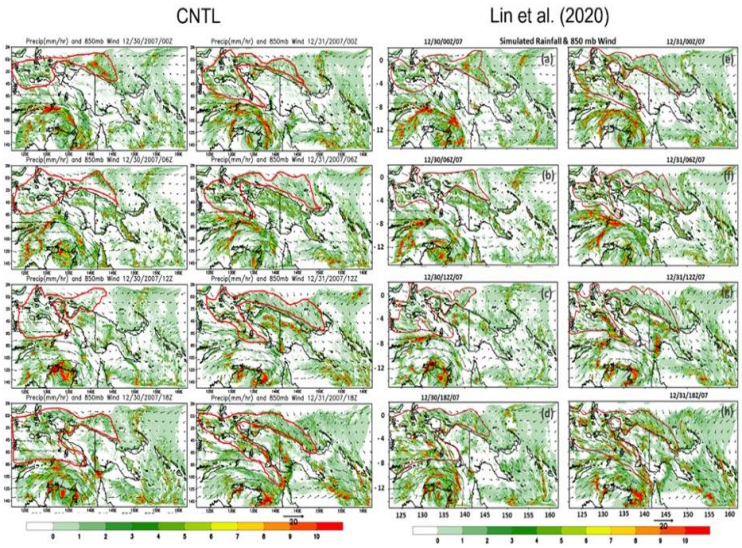

Fig. 2. Simulated rainfall fields (12/30/00Z – 12/31/18Z 2007) in (a) CNTL (left panel) and (b) Part I (Lin et al., [11]) (right panel)

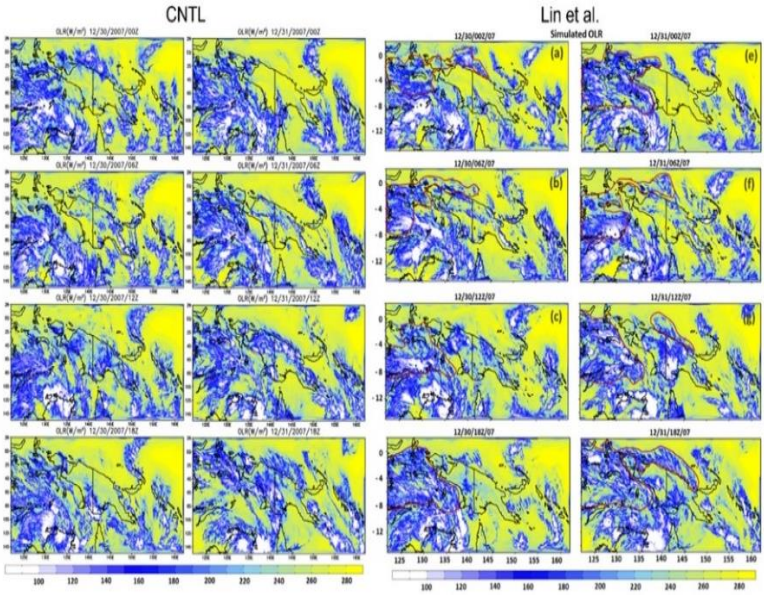

Fig. 3. WRF-simulated OLR fields (12/30/00Z – 12/31/18Z 2007) in (a) CNTL (left panels) and (b) Part I (Lin et al. [11]) (right panels)

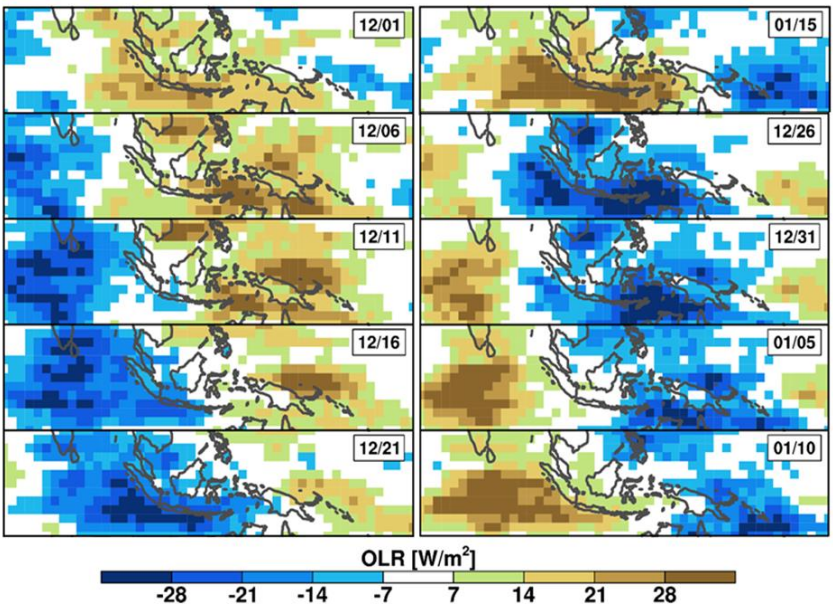

Fig. 4. A Hovmöller (Delayed regression time series) diagram of OLR anomalies (in W m^{-2}) between 15N-15S from Dec. 2007–Feb. 2008. The time interval is 5 days with time increases downward (Gottschalck et al. [24]). Day 0 corresponds to Jan. 2, 2008 (Jiang [23])

convective system, thus entering the *merging stage*. At this stage, the convective system resumes its original MJO system and continues moving southeastward. The NoMT case will be used to show whether the MJO07-08 is able to goes through these stages or not and how much it is being affected by the NGH mountains. We will also inspect how the MJO-rain is affected by the NGH. Based on the NoMT case, we will examine the rainfall change associated with the MJO affected by removing the NGH.

The second sensitivity test is to remove the diurnal heating (NoHT), which allows us to study the impacts of diurnal heating and cooling on the MJO07-08 as it propagates over the NGH. This sensitivity test will isolate the MC's barrier effects on the MJO propagation, which is sometimes seen when the MJO propagates through the MC. We will also look at the sea and land breeze impacts on the MJO and its associated rainfall change. The sensitivity test will also help us differentiate these two forcings and the relative impact on the MJO. The fundamental dynamics is that the mechanical blocking plays a larger role than the thermal forcing.

The final sensitivity test is to remove both the mountain and diurnal heating case (NMNH). The above three sensitivity tests are summarized in Table 2.

Table 2. The control and all the sensitivity cases performed in this study

Case	Key Properties
CNTL	This serves as the control case, which is initialized by the ECMWF-interim data with SST updated every 6 hrs.
NoMT	Same as the CNTL case, except the mountains are removed.
NoHT	Same as the control case, but there is no diurnal heating and cooling in the WRF simulation.
NMNH	No mountains and No diurnal heating and cooling
87.5MT*	Same as the CNTL case, except the mountains are reduced to 87.5% of their original heights.
75MT	Same as the 87.5MT* case except for 75% reduction.
62.5MT*	Same as the 87.5MT* case except for 62.5% reduction.
50MT	Same as the 87.5MT* case except for 50% reduction.
37.5MT*	Same as the 87.5MT* case except for 37.5% reduction.
25MT	Same as the 87.5MT* case except for 25% reduction.
12.5MT*	Same as the 87.5MT* case except for 12.5% reduction.

** The sensitivity tests used for the Froude number discussions.*

3.1 Impact of Mechanical Forcing on MJO07-08

Generally speaking, there exist four types of rain associated with the MJO07-08 in the current situation: (1) MJO-Rain: the rain is originally associated with the MJO before encounters the NGH, (2) Oro-Rain: the rain is mainly caused by the orographic forcing on MJO-Rain, (3) Therm-Rain: the rain is thermally forced by near-surface radiation, and (4) TC-Rain: the rain is mainly associated with the TC-Elizabeth located to the south of the New Guinea island. Note that there are nonlinear interactions among these four types of rain, thus it is almost impossible to clearly distinguish them. In other words, the rainfall on the island is not a simple superposition of any of these four types of rain.

The NoMT case was performed to see how much of an impact the mechanical forcing of the NGH has on MJO07-08. At first glance, when comparing the CNTL case to the NoMT case (Fig. 5), we can see a clear difference in how the MJO interacts with the island when there is no mountain compared to when the NGH is in the domain. When comparing these two cases, one notices the significant differences in the wind flow direction during its passage over NGH. In the NoMT case, the airflow can pass over the NGH, instead of split to pass around the NGH in the CNTL case (Fig. 5). Without obstructing the mountains in the NoMT case, the airflow can move passing the New Guinea island almost freely without being blocked by the mountains. At 00Z/12/31/07, the lack of rainfall in CTRL case is due to that the MJO convection are split into two convective system (Fig. 5a), while the lack of NoMT case (Fig. 5c) is due to surface cooling since the local time is 10 am. On the other hand, at 12Z/12/31/07, the rainfall on the main part of the island in the CNTL case are due to orographic forcing (Fig. 5b), while the rainfall is located on the southeast (SE) peninsula of the New Guinea island in the NoMT case (Fig.

5d) due to surface heating since the local time is 10 am. The propagation speed of MJO07-08 has also increased from approximately 5 m s^{-1} in the CNTL case to 9 m s^{-1} in the NoMT case.

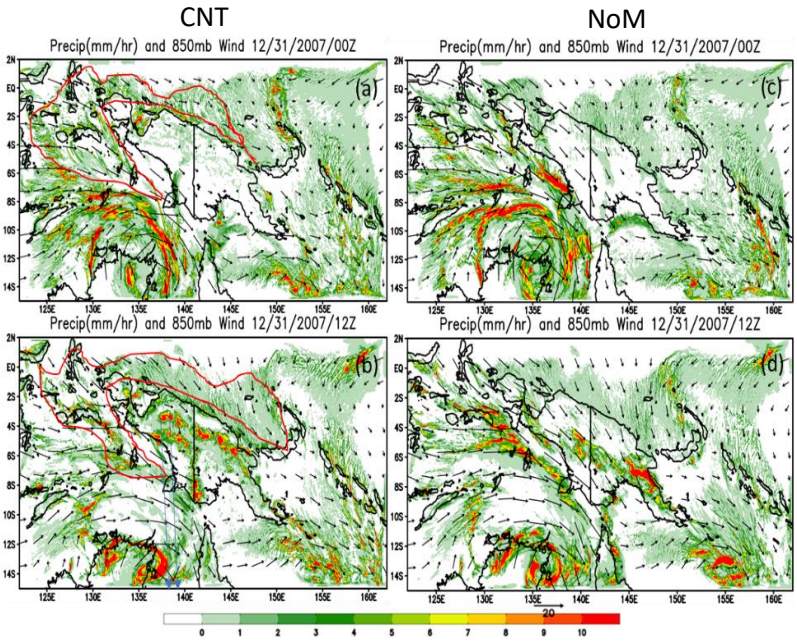

Fig. 5. The 3h rainfall and 850mb wind fields during the *blocking stage* of MJO07-08 (00Z and 12Z, 12/31/07). Panels (a)-(b) and (c)-(d) are for the CNTL and NoMT cases, respectively.

The NoMT case also shows how much the mechanical forcing of the NGH impacts the rainfall associated with MJO07-08. In the NoMT case, there is not much orographic rainfall and clouds over the main part of the island (Figs. 5c and 6c) due to the lack of orographic mechanical forcing associated with the NGH. This does reduce the amount of rainfall over the main part of the island in the NoMT simulation, however, a close look at the rainfall distribution at 12Z, 12/31/07 does show there is a rainfall and clouds increase on the southwest (SW) peninsula of the island (Figs. 5d and 6d) compared to the CNTL case (Figs. 5b and 6b). This is attributed to the convergence of winds that pass over the island due to diabatic surface heating since the local time is 10 pm (UTC+10h).

Fig. 6 shows the simulated OLR fields at 00Z and 12Z, 12/31/07 for CNTL and NoMT cases. At 00Z, there are almost no clouds over the New Guinea island, which is consistent with the rainfall fields (Fig. 5a and 5c). Like the explanation of lack of rainfall in CNTL case earlier, the lack of convective clouds over the New

Guinea island (Fig. 6a) is caused by the lack of MJO convective clouds (Fig. 6c) due to flow and MJO splitting by NGH. In the meantime, the lack of convective clouds is due to the diabatic cooling since the local time is 10 am. At 12Z/12/31/07, the deep convective clouds in the CNTL case (Fig. 6b) are generated by mountains, which help produce heavy Oro-Rain (Fig. 5b). On the other hand, the deep convective clouds presence near the northwest corner of the New Guinea peninsula (Fig. 6d) are generated by convergence and surface heating.

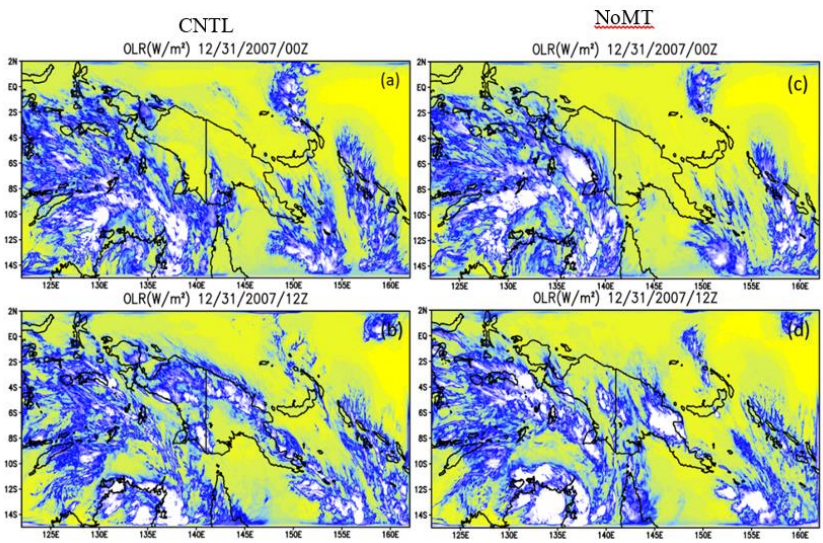

Fig. 6. The OLR fields during the blocking stage of MJO07-08 (00Z and 12Z, 12/31/07). Panels (a)-(b) and (c)-(d) are for the CNTL and NoMT cases, respectively

During the splitting stage, the wind, rain, and convective clouds (Figs. 7 and 8) behave similarly to that during the blocking stage. Thus, they can be explained by the same mechanisms.

3.2 The Impact of Thermal Forcing on MJO07-08

In previous studies, such as Zhang and Ling [8], the heavy rainfall produced by blocking could be caused by the land/sea breeze interaction with the island. However, many of those studies only look at the thermal forcing impacts on the MJO. With the NoHT case, we can isolate the thermal forcing from the mechanical (orographic) forcing of the NGH. If the thermal forcing is shown to play a larger role in the blocking of MJO07-08, this would mean that there would be the presence of a barrier effect around the island. If not, then that would suggest that either the mechanical forcing plays a more dominative role or both mechanical and thermal forcings play comparable role.

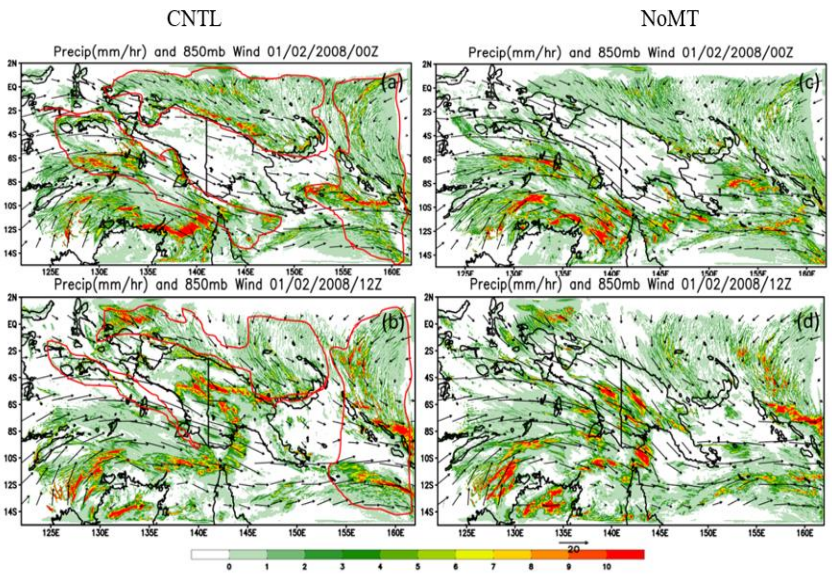

Fig. 7. Simulated 3h rainfall and 850mb wind fields during the splitting stage of MJO07-08 (00Z and 12Z, 1/2/08). Panels (a)-(b) and (c)-(d) are for the CNTL and NoMT cases, respectively

In this study, the impact of the thermal forcing on MJO07-08 is investigated by conducting a case identical to the CNTL case except with the diurnal heating and cooling over the land is deactivated. This sensitivity test is named NoHT case. Comparing the flow fields of CNTL (Fig. 9) and NoHT (Fig. 10), the blocking effect is still present in the NoHT case when the MJO07-08 approaches and interacts with the NGH. However, in the NoHT case, there is only a little orographic rainfall on the island and the mountains due to no sea or land breeze is generated in the simulation. Lin [12] reviews how the complicated interactions between orographic and thermal forcing influence the dynamics of the mountain-plains solenoidal (MPS) circulations. In addition, Lin [12] indicates that sea and land breezes may combine with the orographically and thermally forced winds near the coasts of a mountainous island, including the slope and mountain valley winds. During the day, the mountain serves as an elevated heat source due to the sensible heat released by the mountain surface. Thus, Lin [12] commented that “in a quiescent atmosphere, this can induce mountain upslope flow or upslope wind, which in turn may initiate cumuli or thunderstorms over the mountain peak and produce orographic precipitation." In the CNTL case, the surface temperature and 900 mb wind fields (Fig. 9) show that a sea breeze occurs from 00Z to 12Z (10L to 22L, where L stands for the local time of Papua New Guinea), and there is a land breeze that occurs between from 15Z to 00Z the next day (01L to 10L).

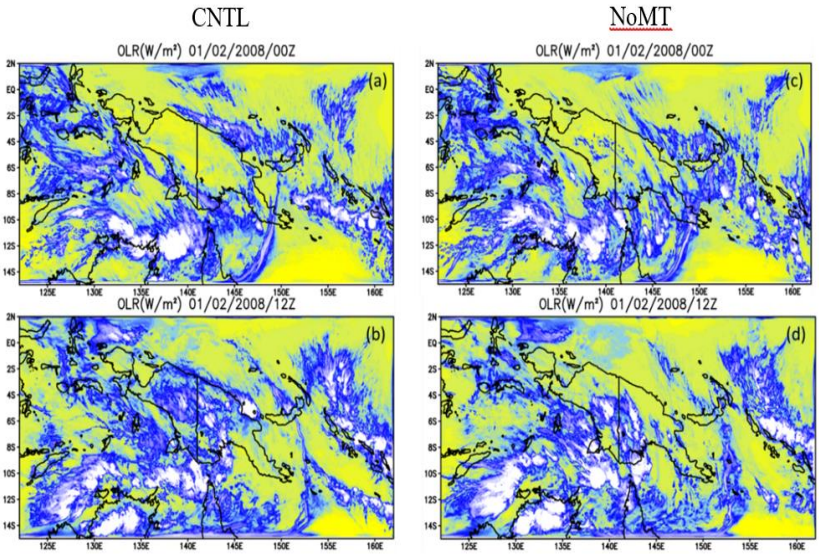

Fig. 8. Simulated OLR fields during the splitting stage of MJO07-08 (00Z and 12Z, 1/2/08). Panels (a)-(b) and (c)-(d) are for the CNTL and NoMT cases, respectively

When the sea breeze interacts with the NGH at the blocking stage, a large amount of rainfall occurs along the NGH corresponds to the strong sea breeze interaction with the NGH (Fig. 11b). On the other hand, during the land breeze interaction, we can see rainfall along the island's coast instead of along the NGH (Fig. 11a). This is like the results observed by Zhang and Ling when discussing the barrier effect for the MJO-B group. Thus, these results in the CNTL show that the thermal forcing from the NGH does play a role in the blocking of MJO07-08.

In the NoHT case, with the removal of the diurnal heating from the land, land breeze cannot be generated, thus plays no roles in generating rainfall (Fig. 11c and 11d). However, since the land remains much cooler than the surrounding ocean water (Fig. 10), sea breeze, though not diurnal, can still be generated and produces rainfall along the coast (Fig. 11d). Because the land is much cooler than the surrounding ocean surface temperature, the thermal forcing associated with the blocking of the MJO is no longer affecting the MJO.

Since there is no sea breeze interaction with the NGH, orographic rainfall has been reduced drastically, but it is still orographic rain being generated along the NGH. This shows that even though there is no longer a sea breeze to help with the production of orographic rainfall due to orographic lifting. Also, when looking at the rainfall off the island's coast, where we saw the land breeze interaction, the rainfall has been drastically reduced. This shows that the barrier effect has strengthened

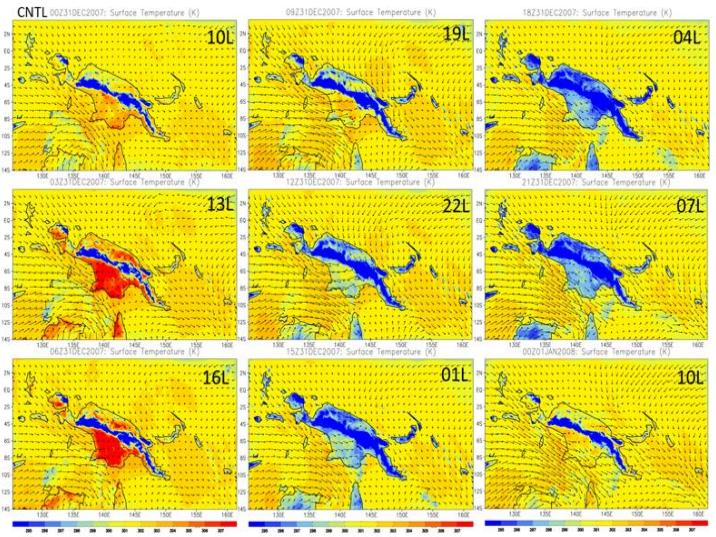

Fig. 9. The 3-hourly surface temperature and 900 mb sigma-pressure (σ-p) wind fields from 12/31/07/00Z(10L) to 1/1/08/00Z(10L) for the CNTL case. L represents the local time on the island (UTC+10h)

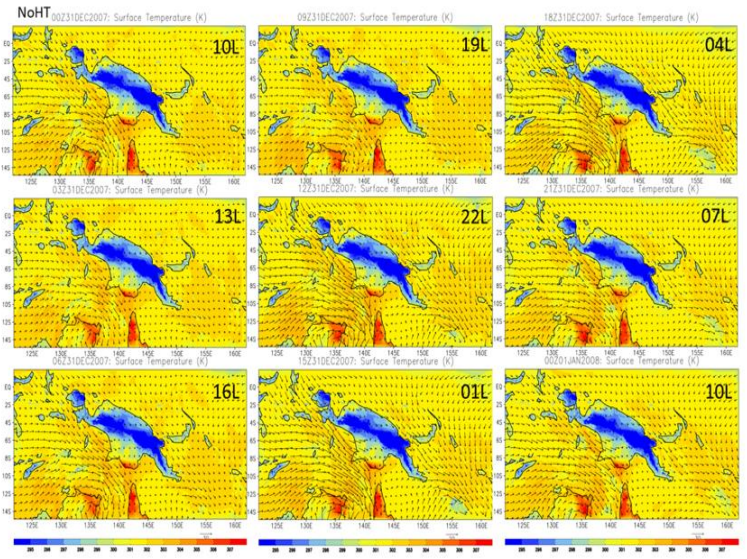

Fig. 10. The 3-hourly surface temperature and 900 mb sigma-pressure (σ-p) wind fields from 12/31/07/00Z(10L) to 1/1/08/00Z(10L) for the NoHT case. L represents the local time on the island (UTC+10h)

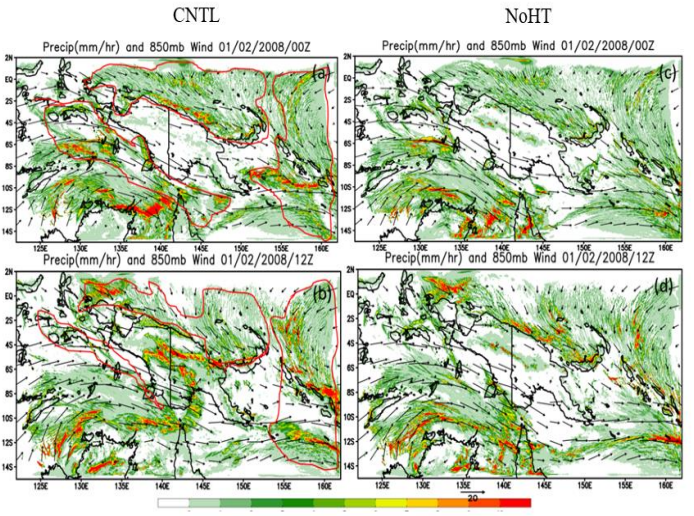

Fig. 11. The 3-h rainfall and 850 mb wind files during the splitting stage of MJO07-08 (00Z and 12Z, 1/2/08). Panels (a)-(b) and (c)-(d) are the CNTL and NoHT cases, respectively

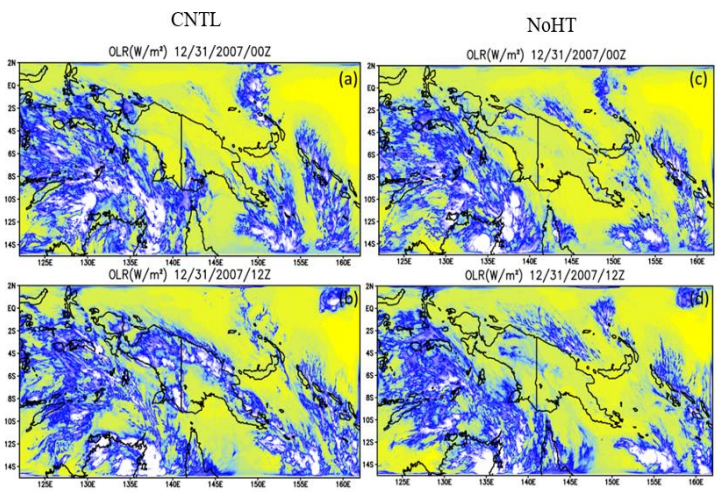

Fig. 12. The OLR fields during the blocking stage of MJO07-08 (00Z and 12Z, 12/31/07). Panels (a)-(b) and (c)-(d) are the CNTL and NoHT cases, respectively

with removing the diurnal heating of the land. This also can be explained when looking at the 850 mb wind fields (Fig. 11) and the OLR figures (Fig. 12). There we

can see that the winds caused the deep convection of MJO07-08 to stay farther from the coast compared to the CNTL and NoMT cases, respectively.

When the diurnal heating and cooling is deactivated, orographic rainfall is still being generated along the NGH. This implies that both mechanical and thermal forcing do play roles in the blocking and splitting of MJO07-08, with the mechanical forcing playing a larger role than the thermal forcing.

3.3 The Impact of Combined Mechanical and Thermal Forcing on MJO07-08

The impact of combined mechanical and thermal forcings is studied by conducting a sensitivity test with both the mountains removed and sensible heating/cooling deactivated (NMNH case). In NMNH, as anticipated, MJO07-08 propagates along with the northwesterly flow and does not interact with the island (Fig. 13). There is no significant orographic rainfall can be seen on the island during the periods when there exist interactions between sea breeze and orography. There is also no rainfall along the coast during the times we would see the land breeze interaction. In addition, the MJO07-08 does not go through any of the stages that are described in Part I [11]. The MJO07-08 system can easily propagate across the NGH at a comparable propagation speed to that of the NoMT case. The NMNH case shows the importance of the thermal and mechanical forcing when it comes to the blocking and splitting MJO07-08. Also, there is no orographic rainfall or other types of rainfall on the island. This lack of rainfall over the land is due to the lack of sea breeze during the simulation. In other words, the absence of diurnal heating/cooling and orographic blocking causes the MJO normally as if there is no landmass interacting with the convective system. Some convergence can be seen on the SW corner of the island. This is due to the weakened sea breeze interacting with the incoming flow from the east. Because the incoming flow is much stronger than the sea breeze, convergence is formed at the SW corner.

Based on the comparison between the sensitivity tests and CNTL case, we found that the thermal forcing itself is not strong enough to block the eastward propagation of MJO07-08 completely. This suggests a very weak barrier effect around the island of New Guinea, which means that the thermal forcing does not play a significant role in generating heavy orographic rainfall. However, this does not mean that thermal forcing does not contribute to heavy rainfall production either. When looking at the NoHT case, we can see that the mechanical forcing of the NGH by itself is strong enough to block the propagation of MJO07-08 completely.

When looking at the OLR Hovmöller diagram (Fig. 14), we can see that even when the thermal forcing is removed from the simulation, there is still strong blocking happening in the environment. This would mean that the mechanical forcing of NGH has a significant impact on the production of orographic rainfall. However, when looking at the three-hourly rainfall plots (Figs. 11c and 11d) we can see that the amount of orographic rainfall has been reduced when the thermal forcing has been removed. This suggests that a combination of mechanical and thermal forcing is needed to produce orographic rainfall in the case of MJO07-08, with the mechanical forcing of the NGH playing a larger role in the orographic rainfall production than the thermal forcing.

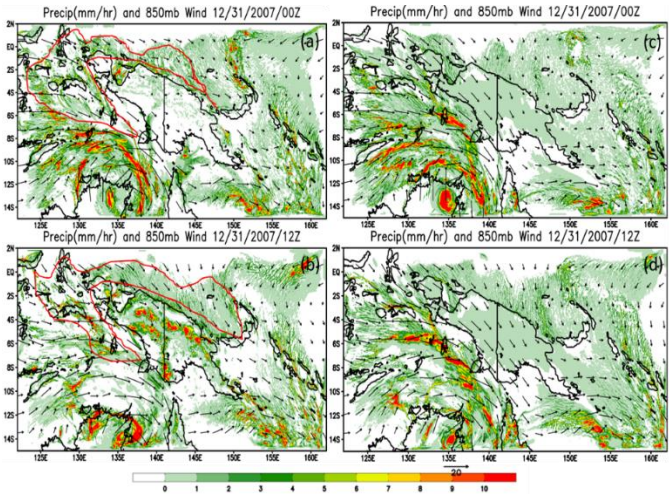

Fig. 13. The 3-h rainfall and 850mb wind fields during the *blocking stage* of MJO07-08 (00Z and 12Z, 12/31/2007). Panels (a)-(b) and (c)-(d) are for the CNTL and NMNH cases, respectively

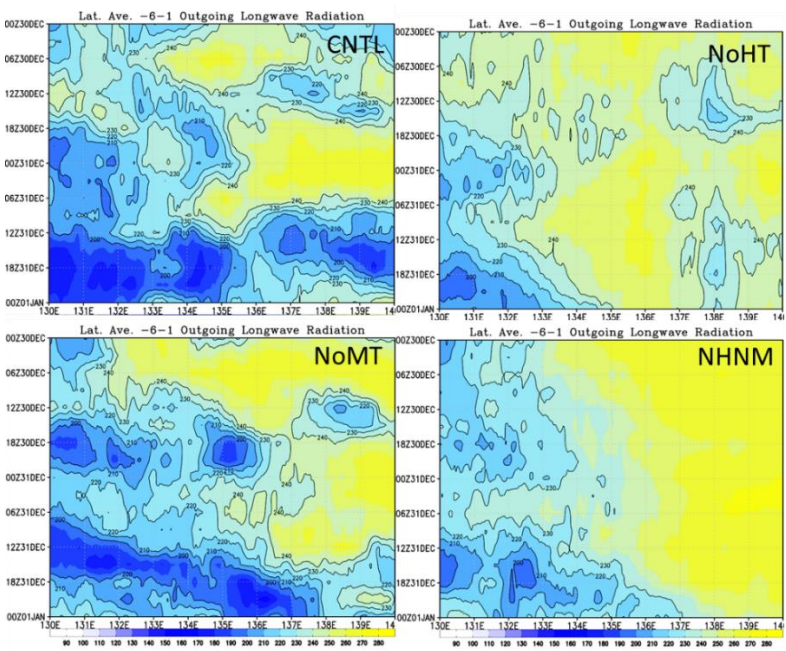

Fig. 14. Hovmöller diagram of OLR fields from 12/30/07 00Z to 1/1/08 00Z for cases CNTL, NoHT, NoMT, and NMNH

4. MODIFICATION OF OROGRAPHIC RAIN ASSOCIATED WITH MJO07-08 PASSING OVER THE NGH

Before discussing the modification of the orographic rain associated with MJO07-08, we found it is necessary to distinguish the following three types of rain: (1) MJO-Rain, which is the rain associated with the MJO. (2) Oro-Rain, which is the rain caused by the mountain's diurnal heating. (3) TC-Rain is the rain associated with the tropical cyclone Elizabeth located south of the island of Papua New Guinea. For this study, we are not worried about the TC-Rain that occurs during the MJO07-08 case. However, we do need to count the TC-Rain out because Tropical Cyclone Elizabeth did occur at the same period when the MJO was propagating over the island. Therefore, our research is only focused on the first two types of rain.

When looking at the enhancement of the orographic rain associated with MJO07-08 passing over the NGH, we can look at the flow regimes and orographic ingredients associated with the blocking stage. The CNTL and NoMT result from the previous section so there is orographic blocking in the NW corner of the NGH during the blocking and splitting stages. To investigate how the orographic rainfall is modified, we will look at the flow regimes of the precipitating system and the orographic ingredients associated with the MJO07-08.

To differentiate the *flow-around* and *flow-over* three-dimensional (3D) flow regime, a slope analysis of the NGH is performed to show when the orographic rain is associated with the MJO07-08 transition between three-dimensional flow and two-dimensional flow. To perform the slope analysis, several simulations are done with varying heights, which are summarized in Table 2. With these varying heights, we calculated the Froude number for each of the cases represented in Table 3 using the equation below, where U is the basic flow speed, N_w is the unsaturated Brunt-Vaisala frequency, and h is the mountain height.

$$F_w = \frac{U}{N_w h} \tag{2}$$

We also used the NoMT case for comparison, even though the Froude number of the NoMT case would be infinite. We calculated the aspect ratio based on Eq. (2) for each case to determine the flow regimes for each case. The *aspect ratio* is denoted as S because it represents the slope of the mountain,

$$S = \frac{h}{L} \tag{3}$$

where h is the mountain height and L is the horizontal distance.

Table 3. The upstream Froude numbers, aspect ratios and flow regimes of sensitivity tests performed

Case	Froude Number (F_w)	Mountain Aspect Ratio (h/L)	Flow Regime
CNTL	0.244	0.060	Flow-around
87.5MT	0.279	0.052	Flow-around
75MT	0.325	0.045	Flow-around
62.5MT	0.390	0.038	Flow-around
50MT	0.488	0.030	Flow around/over
37.5MT	0.651	0.023	Flow-over
25MT	0.976	0.015	Flow-over
12.5MT	1.950	0.008	Flow-over
NoMT	∞	0	Flow-over

This process is like that performed by Chen and Lin [17]. However, there are some key differences when comparing their study to ours. The first difference is that we are only looking at two flow regimes instead of the four flow regimes Chen and Lin [17] found. Second, the way the aspect ratios are found differs from that in their study, which used varying half-widths. However, in this study, we vary the mountain height instead. Finally, Chen and Lin [17] used an idealized mountain to conduct their study. However, in this study, the mountains considered are real mountains. In other words, we are dealing with two flow regimes associated with flow over 3D mountains, i.e. *flow-around and flow-over regimes*. Also, because our mountain is real, our aspect ratio is approximately represented by Eq. (3). The *flow-around regime* can be described as when the MJO becomes blocked during the blocking stage (00Z-12Z, 12/31/2007). The convective system begins to split around the mountain to continue its eastward propagation. This splitting is the same as what is described during the splitting stage described in Part I [11]. The *flow-over regime* is described as when the orographic terrain blocks the MJO. The blocking effect is weak enough that the convective system continues over the mountain instead of splitting around the mountain.

In this study, we calculated the Froude number for each of the cases with varying mountain heights, which is represented in Table 3 using the equation below, where U is the basic flow speed, N_w is the unsaturated Brunt-Vaisala frequency, and h is the mountain height. We also used the NoMT case for comparison, even though the Froude number of the NoMT case would be infinite. We calculated the aspect ratio (Eq. 2) for each case to compare to determine the flow regimes for each case. Where h is the mountain height and L is the horizontal distance. Flow regime flow-over (Regime I) is seen when the mountain height is below 50% of the original mountain height. Flow regime flow-around (Regime II) is seen when the mountain height is above 50% of the original mountain height. When the mountain is at 50% of the original height, the flow regime is in both I and II. This means that we can see the MJO07-08 split around the NGH and flow-over the NGH as well. This shows that the splitting occurs as the orographic terrain blocks the MJO07-08, mostly caused by the terrain itself and not by the terrain's diurnal thermal forcing. This is the opposite of what is discovered in Zhang and Ling [8], which discusses

the barrier effect to the island's thermal forcing. This does not mean their finds are wrong, but this barrier is not the main reason for the flow splitting regarding the NGH and the MJO07-08. In the case of the MJO07-08, the splitting of the convective flow is mainly caused by the mechanical forcing of the mountains.

5. ESSENTIAL INGREDIENTS OF HEAVY OROGRAPHIC RAINFALL ASSOCIATED WITH MJO07-08 PASSING OVER NGH

As discussed briefly in the introduction of this study, Lin et al. (2001) formulated an equation, i.e. Eq. (1), that applied Doswell et al.'s [25] ingredients approach to the upslope of orographic precipitation and proposed several common synoptic and mesoscale environment features favorable to heavy orographic rainfall. Lin [11] identifies that the occurrence of heavy orographic precipitation needs a combination of any of the following ingredients: (1) high precipitation efficiency (ε), (2) strong orographic lifting (w_{oro}) or LLJ (U) and steep mountain ($\partial h/\partial x$) since $w_{oro}=\partial h/\partial x$, (3) strong environmental lifting (w_{env}) (conditional instability associated with large CAPE, potential instability, low-level convergence, upper-level divergence, etc.), (4) large moist airflow upstream (q_v), (5) large preexisting convective system (L_s), and (6) slow translational motion of the storm (c_s). With the MJO07-08 being an MCS that slowly propagates over the NGH, we can confirm that the last two ingredients, the large preexisting convective system and the slow translational motion of the storm, are important ingredients to the production of orographic rainfall.

In investigating whether there is w_{oro} associated with the MJO propagating over the NGH, we check to see if the high mountain or steepness of the orography of the NGH is enough to produce orographic rainfall. The slope is estimated by using the mountain slope represented in the 5 km grid resolution of the simulation. The selected area's slope: the NW corner of the island of New Guinea, is ~ 0.060 (3.5km/58km), which is considered a steep mountain slope to produce orographic rainfall. This means that w_{oro} is an ingredient for orographic rainfall, as can be verified by Fig. 15, which shows that the amount of rain increases as the steepness of the mountain increases.

Next, we want to see if w_{env} is an ingredient for orographic rainfall associated with MJO07-08. Agyakwah and Lin [26] found that CAPE played an essential role in producing heavy orographic rainfall associated with Typhoon Morakot (2009) over Taiwan's Central Mountain Range. In the case of the MJO07-08, we see a large amount of CAPE, which would cause conditional instability during the blocking stage as the MJO propagates over the NHG (Fig. 16a). This means that CAPE plays a significant role in producing heavy orographic rainfall when the strong w_{env} can lead the airflow to trigger conditional instability, which requires large CAPE and strong lifting of the air parcel to reach level of free convection (LFC). Furthermore, the vapor mixing ratio in the area is about 20 g/kg, where the orographic terrain is blocking the MJO (Fig. 16b). This amount is preferable to produce heavy orographic rainfall, as shown in Agyakwah and Lin [26]

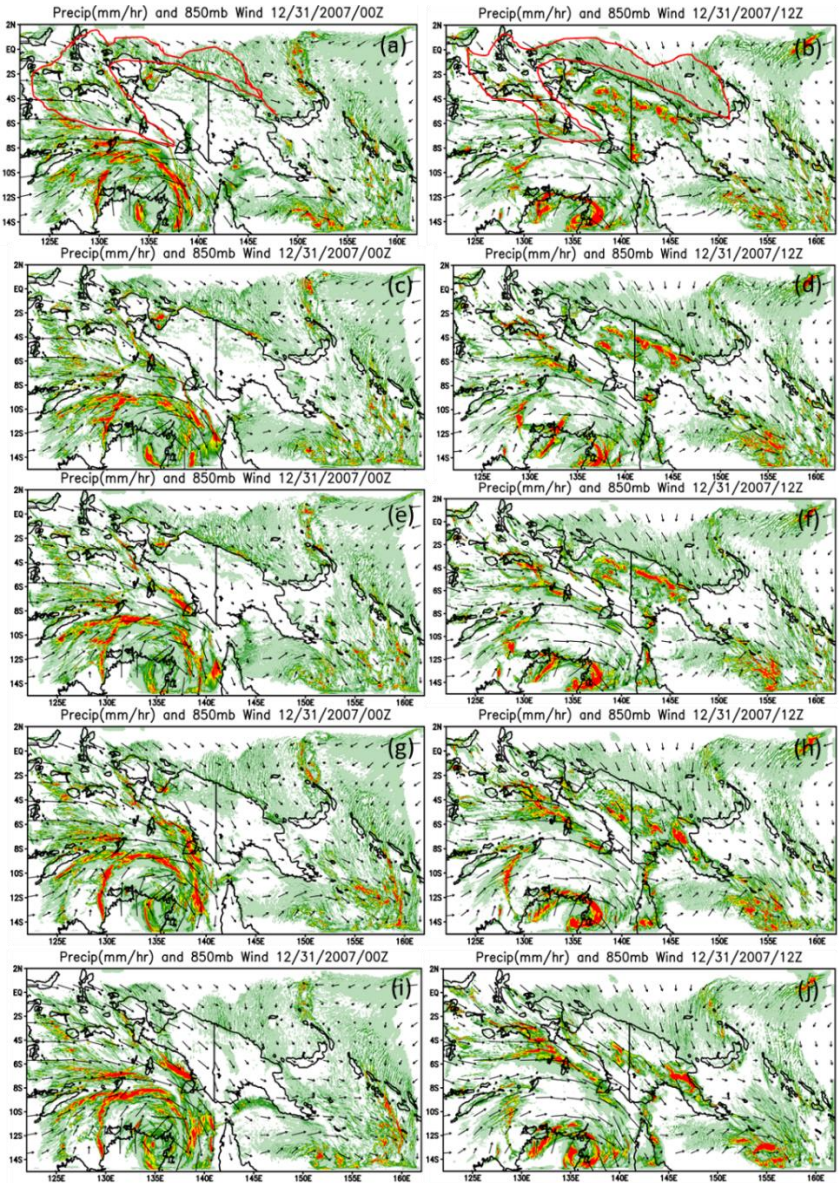

Fig. 15. The 3-h rainfall and 850mb wind fields during the *blocking stage* of MJO07-08 (00Z-12Z, 12/31/07) for each varying height case: CNTL (a,b), 75MT(c,d), 50MT(e,f),25MT (g,h), and NoMT (i,j)

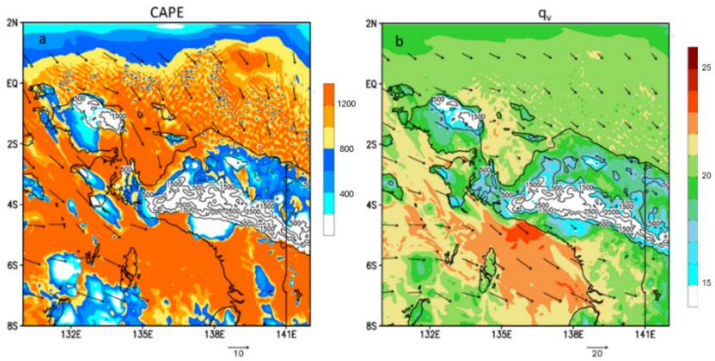

Fig. 16. (a) CAPE calculated from the surface to 850 hPa and (b) water vapor mixing ratio (q_v) for the CNTL case. The units of CAPE and q_v are in J kg^{-1} and g kg^{-1}, respectively

Note that a strong w_{env} may also trigger potential (convective) instability, which requires $\partial q_e/\partial z<0$ (where q_e is equivalent potential temperature) if a layer of atmospheric is lifted, such as a mountain or synoptic front. In addition, in the real atmosphere, the vertical motion (w) cannot be simply decomposed linearly into w_{oro} and w_{env}.

With both w_{oro} and w_{env} serving as ingredients, it is important to investigate which of them plays a larger or more dominant role in the producing orographic rainfall. To do this, we compare the w_{oro} and w_{env} to the total upward motion ($w = w_{oro} + w_{env}$) associated with the MJO07-08 propagating over the NGH (Fig. 17). The result shows that most of the total upward motion associated with the MJO07-08 propagating over the NGH during the blocking stage is caused by the w_{env} and not the w_{oro}. Therefore, these results show that the w_{env} plays a major role in generating orographic rainfall. However, this does not mean that the w_{oro} does not affect the production of orographic rainfall. *Especially, w_{oro} may serve as a necessary and critical mechanism for orographic rain formation, while w_{env} serves as an enhancement mechanism for orographic rain*. These results show that the w_{env} has a much large effect on the production that the w_{oro}. We can also verify these results by looking at the vertical velocity (w) along the NW corner of the island of New Guinea and NGH.

Based on Eq. (1) and assuming the low-level basic wind is U, then it leads to

$$P = \varepsilon \left(\frac{\rho_a}{\rho_w}\right)(V_H \cdot \nabla h + w_{env})\left(\frac{L_s}{c_s}\right) q_v \propto U\, \partial h/\partial x\, q_v. \quad (4)$$

Therefore, when the low-level basic flow is uniform and unidirectional, the total precipitation (P) increases linearly as the upward motion increases. However, this would not occur in the real world since the mountain is normally three dimensional, instead of a 2D ridge. In other words, when the mountain slope or mountain height (with mountain width in flow direction kept constant) increases, the blocking effect becomes stronger, then the low-level basic flow would be forced to go around the

mountain and the orographic precipitation would not keep increasing. That is, the flow will split horizontally, and the total precipitation would start to reduce once a critical mountain slope or mountain height is reached. In terms of convective system, it would split into two systems, like what simulated in the *splitting stage*, and the maximum precipitation on upslope along the center line would decrease [27,28].

Fig. 18 shows the accumulated rainfall for a series of sensitivity experiments CNTL, 75MT, 50MT, 25MT, and NoMT. The corresponding moist Froude numbers are 0.244, 0.325, 0.488, 0.976, and ∞, respectively. Fig. 18 accumulated maximum rainfall on upslope for all cases versus the steepness (h/L_x) or mountain height (with fixed L_x), where is the mountain horizontal scale in the direction of basic flow, which is NW to SE in the current situation. The 3h accumulated maximum rainfall on upslope increases linearly as the mountain height (normalized by the full mountain height of the control case) increases until it reaches 75% mountain height. Once the normalized mountain height reaches above 75%, the propagation of the MJO moves from a flow-over regime to a flow-around regime [29].

To study the strong environmental upward motion associated with the MJO07-08, we also examined the vertical velocity (w) along the NW corner of the island of New Guinea and NGH with mountain height of NGH reduced from the full mountains (CNTL) to 75% (75MT), 50% (50MT), 25% (25MT), and no mountains (NoMT). When looking at the w field for each case (Fig. 19), we can see that during the blocking stage of the MJO07-08 (00Z-12Z, 12/31/07), there is a strong vertical motion off the main island's coast in the CNTL case. When the mountain height decreases, the strong upward motion moves fourth inland. We can also see that there is a strong downward motion located on the island. However, when the mountain height decreases, the strong downward motion mixes with the strong upward motion and reduces the strong downward motion. When looking at the 3-hourly rainfall results shown earlier and comparing the location of orographic rainfall to the strong w, we can see that reducing the strong w causes a reduction in the amount of orographic rainfall along the NGH. The reduction of the strong w also shows that MJO07-08 is transferring into a flow-over flow regime instead of the flow-around flow regimes that were discussed in earlier sections. Because of this transfer into another flow regime, we can see that it reduces the strong w, reducing the amount of orographic rainfall production by the NGH.

There is a strong upward motion (Fig. 19) associated with a strong convergence field near the area of blocking (Fig. 20). There is also strong divergence along the peninsula that is part of the main island. As the mountain height decreases, the strong divergence along the peninsula begins to move inward toward the main island. We can also see that the strong convergence begins to spread along the island's coast as the mountain height decreases. This strong divergence means reducing the amount of orographic rainfall produced as the moist air is lifted upward along the mountain [30]. With these ingredients, we can confirm that that mountain high, the mountain's shape, and the strong w are suitable to produce orographic rainfall as MJO07-08 propagates over the NGH. Also, the study results show that reducing the mountain height reduces the strength of the w, which also reduces the amount of orographic rainfall along the NGH.

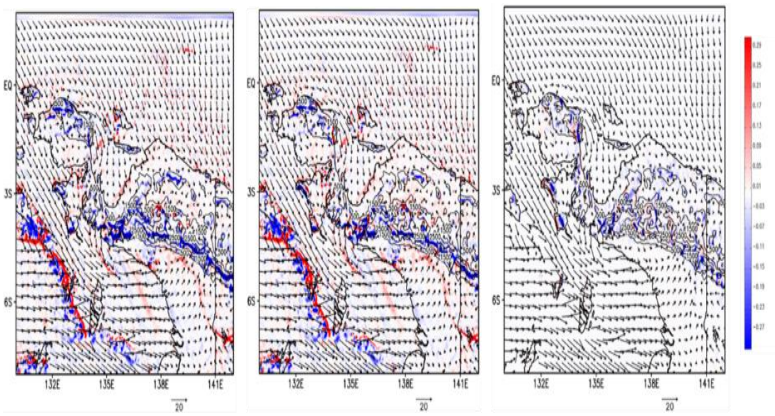

Fig. 17. (a) The total upward motion (*w*) for the NW corner during the blocking stage, (b) the environmental upward motion (w_{env}), and (c) the orographic upward motion (w_{oro})

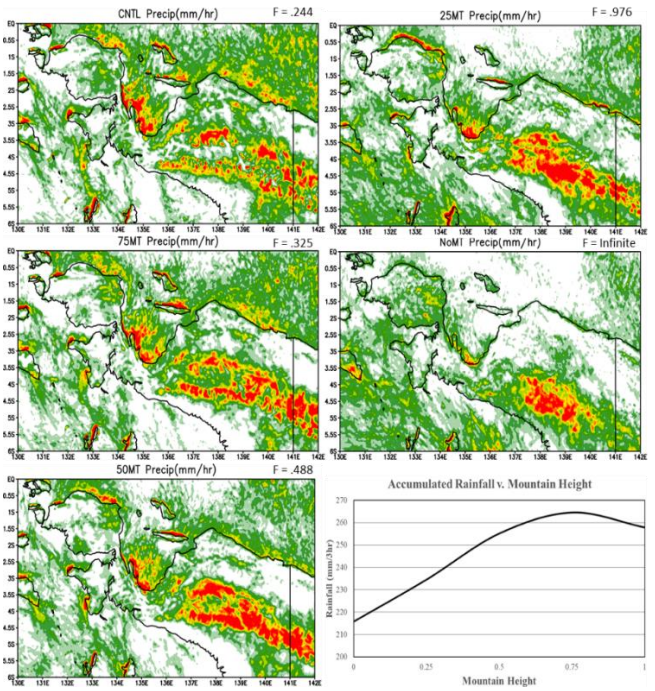

Fig. 18. Accumulated rainfall for cases CNTL, 75MT, 50MT, 25MT, and NoMT. The 3-h accumulated maximum rainfall on upslope rainfall vs. steepness (h/L_x) or normalized mountain height (with fixed L_x) is shown in the lower-right panel

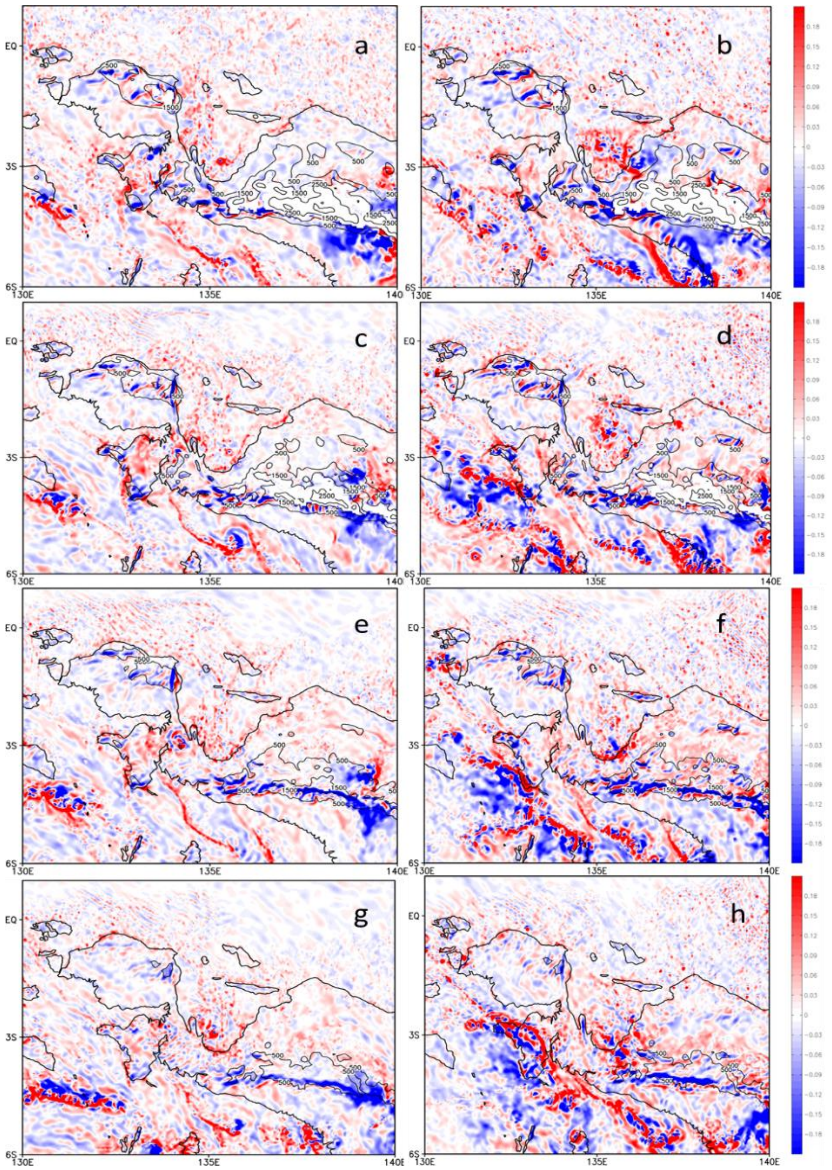

Fig. 19. The vertical motion (*w*) during the blocking stage (00Z-12Z, 12/31/07) for each varying height case: CNTL (a,b), 75MT (c,d), 50MT (e,f), and 25MT (g,h)

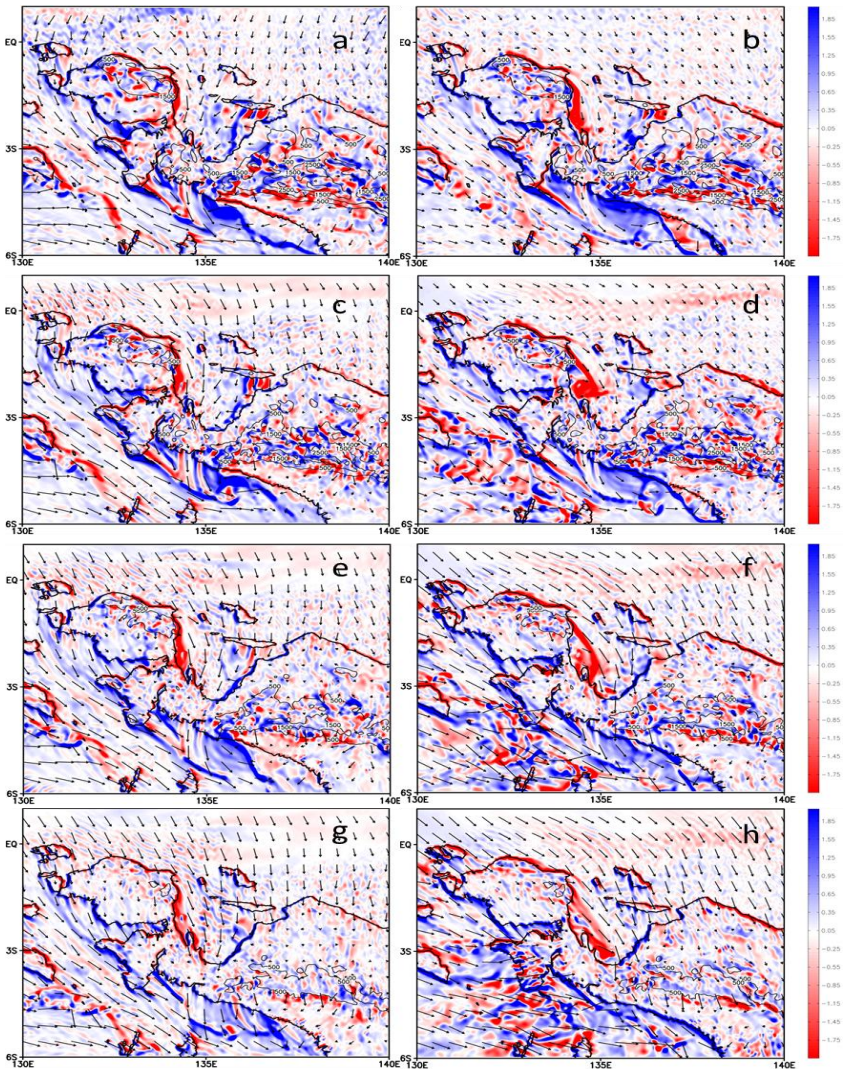

Fig. 20. The convergence and divergence fields (in s^{-1}) during the *blocking stage* (00Z and 12Z, 12/31/07) for each varying height case: CNTL (a,b), 75MT (c,d), 50MT (e,f), and 25MT (g,h)

6. CONCLUDING REMARKS

In this study, we used the Advanced Research Weather Research and Forecasting (WRF) model with systematic experiments to investigate (a) effects of mechanical and thermal forcings on, (b) modification of orographic rain associated with, and

(c) essential ingredients of heavy orographic rainfall associated with MJO07-08 during its passage over New Guinea Highlands (NGH).

First, effects of mechanical and thermal forcings on the NGH are examined by removing the mountains (NoMT), deactivating diurnal heating and cooling (NoHT), and removing mountains and deactivating diurnal heating and cooling (NMNH). In the NoMT case, the airflow and the MJO can go-over the NGH, instead of going-around the NGH in the CNTL case. The NoMT simulated MJO07-08 moves through the New Guinea island at a speed approximately 9 ms^{-1}, which is much faster than the CNTL simulated speed of 5 ms^{-1} due to lack of blocking by NGH. The diurnal surface cooling appears to suppress the convection in NoMT case, while the diurnal surface heating appears to help generate flow confluence and upward motion to produce rainfall over the southeast peninsula of the New Guinea island. It is found that both orographic mechanical forcing and thermal forcing play important roles in generating and modifying rainfall over the NGH and surrounding oceans, with the orographic mechanical forcing playing a stronger role.

Second, a series of systematic sensitivity tests shows that two flow regimes, i.e. flow-around and flow-over regimes, are associated with MJO07-08 during the blocking stage. In the flow-around regime, the convective system associated with the MJO is forced to split around the NGH due to the strong orographic blocking. The flow-around regimes occur when the mountain height is above 50% of the original mountain height. There is also an increase in orographic rainfall as the mountain height increases, and the mountain is seen in the CNTL case. The flow-over regime can be seen when the mountain is below 50% of the original mountain height. The convective system can be seen moving over the NGH with minimum to no blocking from the orographic terrain. When the mountain is at exactly 50%, the convective system can be observed in both the flow-around and flow-over regimes.

Third, based on the common ingredients responsible for heavy orographic rainfall proposed in previous studies, some key ingredients are found for the MJO07-08 passing over the NGH with complex terrain: (1) there needs to be strong vertical motion over the mountain's upslope, (2) there exists high CAPE associated with the airstream, and finally (3) the mountain must be high but not too high. That is, it requires an environmental flow that has a high CAPE flow over a high mountain. On the other hand, if the mountain is too high, then the flow regime could transit from the flow-over to flow-around regime. With a series of sensitivity tests with the mountain height, we found that once the mountain height reaches 75% of the original height of the NGH, the maximum rainfall amount starts to decrease as the mountain height reaches approximately 75% of the original height.

DISCLAIMER (ARTIFICIAL INTELLIGENCE)

The authors hereby declare that NO generative AI technologies such as Large Language Models (ChatGPT, COPILOT, etc) and text-to-image generators have been used during writing or editing of manuscripts.

ACKNOWLEDGEMENTS

This research was supported by the Title III Fellowship, NSF Awards 1900621, and 2022961. In addition, we would like to thank the anonymous reviewers and Drs. L. Liu, A. Mekonnen, and J. Zhang at the North Carolina A&T State University for their valuable comments. Finally, the authors would also like to acknowledge the Computational and Information Systems Laboratory (CISL) of NCAR for their support of computing time on the Cheyenne supercomputer (Project No. UNCS0030). A preliminary version of this study has been published in Earth Sci. Res., 11, 1, 2022.

COMPETING INTERESTS

Authors have declared that no competing interests exist.

REFERENCES

1. Monier E, Weare BC, Gustafson WI. The Madden-Julian oscillation wind-convection coupling and the role of moisture processes in the MM5 model. Climate Dynamics. 200935(2-3):435-447.
   Available:https://doi.org/10.1007/s00382-009-0626-4
2. Hsu H-H, Lee M-Y. Topographic effects on the eastward propagation and initiation of the Madden-Julian Oscillation. Journal of Climate. 2005;18 (6):795-809.
   Available:https://doi.org/10.1175/jcli-3292.1
3. Inness PM, Slingo JM. The interaction of the Madden-Julian Oscillation with the Maritime Continent in a GCM. Quarterly Journal of the Royal Meteorological Society. 2006;*132*(618):1645-1667.
   Available:https://doi.org/10.1256/qj.05.102
4. Wu CH, Hsu HH. Topographic influence on the MJO in the Maritime Continent. Journal of Climate. 200922(20):5433-5448.
   Available:https://doi.org/10.1175/2009jcli2825.1
5. Tseng WL, Hsu HH, Keenlyside N, June Chang CW, Tsuang BJ, Tu CY, Jiang LC. Effects of surface orography and land-sea contrast on the Madden-Julian Oscillation in the Maritime Continent: A numerical study using ECHAM5-SIT. Journal of Climate. 2017;30(23):9725-9741.
   Available:https://doi.org/10.1175/jcli-d-17-0051.1
6. Zhou Y, Wang S, Fang J, Yang D. The Maritime Continent Barrier Effect on the MJO Teleconnections during the Boreal Winter Seasons in the Northern Hemisphere. J. Climate. 2023;36:171-192.
   Available:https://doi.org/10.1175/JCLI-D-21-0492.1.
7. Kim D, Kim H, Lee M. Why does the MJO detour the Maritime Continent during austral summer? Geophysical Research Letters. 2017;44(5):2579-2587.
   Available:https://doi.org/10.1002/2017gl072643
8. Zhang C, Ling J. Barrier effect of the Indo-Pacific Maritime Continent on the MJO: Perspectives from tracking MJO precipitation. Journal of Climate.2017;30(9):3439-3459.
   Available:https://doi.org/10.1175/jcli-d-16-0614.1

9. Ling J, Zhang C, Joyce R, Xie P, Chen G. Possible role of the diurnal cycle in land convection in the barrier effect on the MJO by the Maritime Continent. Geophysical Research Letters. 2019;46(5):3001-3011. Available:https://doi.org/10.1029/2019gl081962
10. Bai H, Schumacher C. Topographic Influences on Diurnally Driven MJO Rainfall Over the Maritime Continent. J. Geophys. Res: Atmosphere, 2022;127:6. Available:https://doi.org/10.1029/2021JD035905
11. Lin Y-L, Agyakwah W, Riley J. G, Hsu HH, Jiang LC. Orographic effects on the propagation and rainfall modification associated with the 2007-08 Madden-Julian oscillation (MJO) past the New Guinea Highlands. Meteorology and Atmospheric Physics. 2020;133(2):359-378. Available:https://doi.org/10.1007/s00703-020-00753-2
12. Lin Y-L. Mesoscale dynamics. Cambridge University Press. 2010:630.
13. Chu CM, Lin YL. Effects of orography on the generation and propagation of mesoscale convective systems in a two-dimensional conditionally unstable flow. Journal of the Atmospheric Sciences. 2000;57(23):3817-3837. Available:https://doi.org/10.1175/1520-0469(2001)057<3817:eoootg>2.0.co;2
14. Chen SH, Lin YL. Effects of moist Froude number and CAPE on a conditionally unstable flow over a mesoscale mountain ridge. Journal of the Atmospheric Sciences. 2005b;62(2):331-350. Available:https://doi.org/10.1175/jas-3380.1
15. Emanuel KA. Atmospheric convection. Oxford University Press. 1994:580.
16. Huang YC, Lin YL. A study on the structure and precipitation of Morakot (2009) induced by the Central Mountain Range of Taiwan. Meteorology and Atmospheric Physics. 2013;123(3-4):115-141. Available:https://doi.org/10.1007/s00703-013-0290-4
17. Chen SH, Lin YL, Zhao Z. Effects of unsaturated moist Froude number and orographic aspect ratio on a conditionally unstable flow over a mesoscale mountain. Journal of the Meteorological Society of Japan. Ser. II. 2008;86(2):353-367. Available:https://doi.org/10.2151/jmsj.86.353
18. Miglietta MM, Rotunno R. Numerical simulations of conditionally unstable flows over a mountain ridge. Journal of the Atmospheric Sciences. 2009 66(7):1865-1885. Available:https://doi.org/10.1175/2009jas2902.1
19. Smolarkiewicz PK, Rotunno R. Low Froude number flow past three-dimensional obstacles. Part I: Baroclinically generated lee vortices. Journal of the Atmospheric Sciences. 1989;46(8):1154-1164. Available:https://doi.org/10.1175/1520-0469(1989)046<1154:lfnfpt>2.0.co;2
20. Buzzi A, Tartaglione N, Malguzzi P. Numerical simulations of the 1994 Piedmont Flood: Role of orography and moist Processes. Monthly Weather Review. 1998;126(9):2369-2383. Available:https://doi.org/10.1175/1520-0493(1998)126<2369:nsotpf>2.0.co;2

21. Skamarock WC, Klemp JB, Dudhia J, Gill DO, Liu Z, Berner J, Wang W, Powers JG, Duda MG, Barker DM, Huang XY. *A Description of the Advanced Research WRF Model Version 4*. UCAR/NCAR; 2019. Available:https://doi.org/10./1DFH-6P97
22. Dee P, Uppala SM, Simmons AJ, Berrisford P, Poli P, Kobayashi S, Andrae U, Balmaseda MA, Balsamo G, Bauer P, Bechtold P, Beljaars ACM. L. van de Berg, Bidlot J. The ERA-Interim reanalysis: Configuration and performance of the data assimilation system; 2011. Available:https://doi.org/10.1002/qj.828
23. Jiang LC. The interaction between the MJO and topography: Using high-resolution data. Master Thesis, Department of Atmospheric Sciences, National Taiwan University. 2012:82.
24. Gottschalck J, Zhang Q, Wang W, L'Heureux M, Peng P. MJO monitoring and assessment at the Climate Prediction Center and initial impressions of the CFS as an MJO forecast tool. NOAA CTB–COLA Joint Semin.2008:15-22. Available:http://www.nws.noaa.gov/ost/climate/STIP/
25. Doswell CA, Broks HE, Maddox RA. Flash flood forecasting: An ingredients-based methodology. Weather and Forecasting. 1996;11(4), 560-581. Available:https://doi.org/10.1175/1520-0434(1996)011<0560:fffaib>2.0.co;2
26. Agyakwah W, Lin YL. Generation and enhancement mechanisms for extreme orographic rainfall associated with Typhoon Morakot over the Central Mountain Range of Taiwan. Atmospheric Research. 2021;247:105160. Available:https://doi.org/10.1016/j.atmosres.2020.105160
27. Chen SH, Lin YL. Orographic effects on a conditionally unstable flow over an idealized three-dimensional mesoscale mountain. Meteorology and Atmospheric Physics. 2005a;88(1-2):1-21. Available:https://doi.org/10.1007/s00703-003-0047-6
28. Chiao S, Lin YL. Numerical modeling of an orographically enhanced Precipitation event associated with Tropical Storm Rachel over Taiwan. Weather and Forecasting. 2003;18(2):325-344. Available:https://doi.org/10.1175/1520-0434(2003)018<0325:nmoaoe>2.0.co;2
29. Rostom R, Lin YL. Common ingredients and orographic rain index (ORI) for heavy precipitation associated with tropical cyclones passing over the Appalachian Mountains. Earth Science Research. 2021;10(1):32. Available:https://doi.org/10.5539/esr.v10n1p32
30. Witcraft NC, Lin YL, Kuo YH. Dynamics of orographic rain associated with the passage of a tropical cyclone over a mesoscale mountain. Terrestrial, Atmospheric and Oceanic Sciences. 2005;16(5):1133. Available:https://doi.org/10.3319/tao.2005.16.5.1133(a)

Biography of author(s)

Justin G. Riley
North Carolina A&T State University, Greensboro, North Carolina, USA and NOAA Cooperative Institute for Great Lakes Research (CIGLR), Ann Arbor, Michigan, USA.

He is a postdoctoral fellow working with CIGLR and GLERL on the Lake Ontario Bipartisan Infrastructure Law (BIL) Coastal and Inland Flood Inundation Mapping (CIFIM) Project. Prior to working with CIGLR, he studied the effects of orographic terrain on extreme weather events like the Madden-Julian Oscillation and the wildfires in the mountains of California.

Yuh-Lang Lin
North Carolina A&T State University, Greensboro, North Carolina, USA

He is a professor at Physics Department and Applied Science and Technology Ph.D. Program, North Carolina A&T State University. He teaches courses covering atmospheric dynamics and modeling and he has published more than 140 articles on Mountain Meteorology, Moist Convection, Wildfire Dynamics, Numerical Weather Prediction, Tropical Cyclone Dynamics, and Cloud Microphysics Parameterizations (with 9627 citations on Google Scholar & listed as World's top 2% scientists by Stanford U. in 2020).

DISCLAIMER
This chapter is an extended version of the article published by the same author(s) in the following journal.
Earth Science Research, 11(1): 25-46, 2022. DOI: 10.5539/esr.v11n1p25

Peer-Review History:
This chapter was reviewed by following the Advanced Open Peer Review policy. This chapter was thoroughly checked to prevent plagiarism. As per editorial policy, a minimum of two peer-reviewers reviewed the manuscript. After review and revision of the manuscript, the Book Editor approved the manuscript for final publication. Peer review comments, comments of the editor(s), etc. are available here: https://peerreviewarchive.com/review-history/296